Large Scale Structures in Nanocomposite Hydrogels

Elena Loizou,[†] Paul Butler,[‡] Lionel Porcar,[‡] Ella Kesselman,[§] Yeshayahu Talmon,[§] Avinash Dundigalla,[†] and Gudrun Schmidt*,[†]

Department of Chemistry, Louisiana State University, Baton Rouge, Louisiana 70803; National Institute of Standards and Technology, Gaithersburg, Maryland 20899; and Technion-Israel Institute of Technology, Haifa 32000, Israel

Received December 16, 2004
Revised Manuscript Received January 31, 2005

The colloidal properties of nanocomposite polymer−clay gels and solutions have received considerable attention in the literature. Unusual properties are induced by the physical presence of the nanoparticle and by the interaction of the polymer with the particle and the state of dispersion. Approaches developed range from manipulation of individual particles to exploitation of self-assembly in colloids.[1,2] The large aspect ratio of platelets promotes a supramolecular organization similar to other mesoscopic systems such as liquid crystalline polymers, surfactants, or block copolymers.

Poly(ethylene oxide) (PEO) absorbs onto clay platelets. Low molar mass polymers thus inhibit aggregation by classic steric hindrance, while higher molar mass polymers, particularly at higher concentrations of clay, bridge between particles and lead to the formation of large clusters[3] or smart gels with novel properties.[4−7] Recent small-angle neutron scattering (SANS) studies describe the adsorption of PEO polymer chains onto Laponite clay platelets at low polymer and clay concentrations using contrast variation methods to separate the contributions from bulk and adsorbed polymer chains.[8,9] These studies showed that the adsorbed polymer layer thickness is about 1.5 nm on each face independent of polymer molecular weight. Even more recently, SANS studies made with no excess polymer confirm these results but also find that the edges of the platelets have polymer density on them that is much thicker than on the face.[10] Other research groups have used neutron diffraction to look at the local segmental, salt, and water structure around each clay platelet and to understand the mechanism of bridging flocculation.[11,12]

Below the threshold for complete saturation of clay particles by sufficiently large molecular weight polymers, "shake gels" can be generated which undergo a dramatic shear thickening when subjected to vigorous shaking.[7] Above this threshold we showed in our previous work that the systems form strong shear thinning gels. In that case, we postulated a dynamic adsorption−desorption equilibrium of the entangled polymer chains with the clay particles to form "permanent" networks.[4−6] Those preliminary data suggest that it is possible to tune gelation as well as kinetics; however, more studies are necessary to quantify results. The purpose of this communication is to describe and correlate microscopic and nanoscopic structures in a polymer clay hydrogel. Several methods have been applied to examine the polymer−clay interactions. Among them, microscopy and light, X-ray, and neutron scattering have proven to be powerful techniques for revealing their structure and providing a measure of size, shape, and interfacial polymer conformation. Here we use a combination of small-angle neutron scattering and microscopy techniques to provide a more complete physical picture of the large scale structure and explain some of the unique behavior observed previously.

In this study aqueous solutions of the synthetic hectorite type clay (Laporte Industries Ltd.), Laponite RD (LRD), and poly(ethylene oxide) (PEO) were used. The clay particles are composed of platelets of high purity and relatively uniform size (30 ± 5 nm in diameter and ca. 1 nm thick) and have a specific surface of 370 m^2/g as estimated by the supplier. PEO with a $M_w = 100 \times 10^3$, 300×10^3, 600×10^3, and 10^6 g/mol was purchased from Polysciences Inc. For all samples in this study a pH value of 10 and a NaCl concentration of 10^{-3} mol/L were used. The results reported here were obtained from gels containing mass fractions of 3% LRD and 2% PEO at room temperature. At equilibrium, the clay surfaces are covered by adsorbed PEO segments with the diffuse polymer chains serving to "bridge" neighboring clay particles, leading to a macroscopically homogeneous transparent hydrogel with clay relatively complete exfoliation as evidenced by a lack of peaks at high q in SANS.[4]

SANS and ultrasmall-angle neutron scattering (USANS) measurements were performed on instruments at the Center for Neutron Research of the National Institute of Standards and Technology (NIST). Both instruments are described well in the literature.[13,14] The scattering data were corrected for background and parasitic scattering and placed on an absolute level using NIST standard procedures. Circularly averaged SANS data yield the scattered intensity $I(q)$ as a function of the wave vector q. Small-angle and ultrasmall-angle scattering investigations are excellent tools in providing quantitative information concerning structures on the 1 to ca. 20 000 nm length scales. A combination of transmission electron microscopy (TEM) and scanning electron microscopy (SEM) provides direct visualization of the nanometer and micron scale structures and can help to clarify their distribution in the system. TEM samples from the polymer clay gel were prepared by the freeze fracture (FF) technique, resulting in a carbon−platinum replica of the fractured sample surface. TEM from a pure Laponite clay solution (<0.1 wt % of clay) is from a vitrified solution and imaged in the frozen state by Cryo-TEM. Environmental scanning electron microscopy, providing a controlled humidity sample environment, was performed with a FEI Quanta 200 environmental SEM instrument. Careful attention was paid to minimize effects from solvent evaporation and condensation. All SEM samples were freeze fractured in Freon to avoid ice crystals formation and the fractured surface imaged directly without use of replicas.

Our current understanding of present and previous results is that the polymer chains are in a dynamic adsorption/desorption equilibrium with the clay particles to form a network. Since there is more polymer

[†] Louisiana State University.
[‡] National Institute of Standards and Technology.
[§] Technion−Israel Institute of Technology.
* Corresponding author. E-mail gudrun@lsu.edu.

10.1021/ma047411a CCC: $30.25
Published on Web 02/24/2005

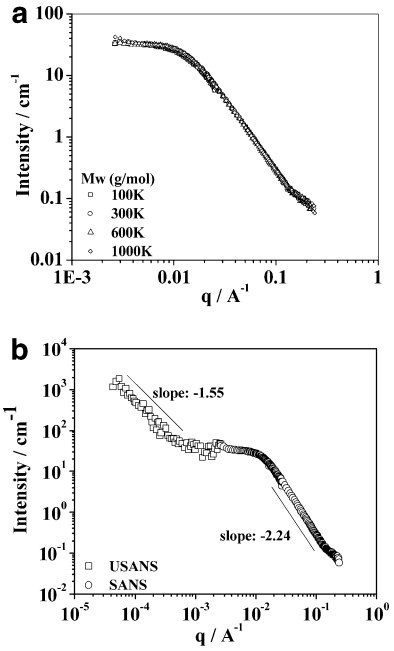

Figure 1. (a) SANS scattering intensity vs q from samples with the same polymer and clay concentration but different polymer M_w. (b) Combined SANS and USANS intensity as a function of Q range for a polymer−clay gel with polymer $M_w = 10^6$ g/mol and at 25 °C. A standard relative error for the SANS data is within 7%.

available than necessary to cover all the clay platelets, we expect the presence of excess polymer may influence the network structure and will certainly affect the scattering patterns. The scattering and microscopy results presented here confirm that polymer−clay gels contain structures on a multiple length scale.

Figure 1a shows SANS data for several different molecular weights (M_w) in the q range of ($q = 4\pi/\lambda \sin(\theta)/2$), 2.27×10^{-3} Å$^{-1} < q < 0.24$ Å^{-1}. The data clearly show the complete lack of M_w dependence in this q regime which probes length scales up to slightly larger than an individual disk. This is consistent with the findings of Lal et al.[8,9] and Nelson et al.[10] that the adsorbed polymer layer thickness is independent of molecular weight and with the fact that scattering from a polymer network above c^* is also independent of molecular weight. The slope at high q of slightly more than the $-2(q^{-2})$ expected for disklike structures is not surprising given that the free polymer coils also must contribute some to the scattering in this regime.[15−17] An apparent R_g can be obtained from a Guinier fit to the data and yields ca. 10 nm consistent with the R_g of 10.6 nm for 30 nm diameter disks. However, attempts to fit the full curve to a core + shell model similar to Nelson et al.[10] for dilute systems of PEO/Laponite fails.

Figure 1b displays combined SANS and USANS intensity profiles covering a much larger q range of 4.36×10^{-5} Å$^{-1} < q < 0.33$ Å^{-1} for a single molecular weight of $M_w = 10^6$ g/mol. With the additional q range it becomes clear that larger scale structures exist in the solution which is not surprising given our "bridged" clay network model. If one assumes the larger scale structure is in fact due to the clay network rather than pure polymer or some other entity, the observed slope of 0 seen between the very low and very high q (slopes of −1.55 and −2.24, respectively) is likely a convolution of the low q part of the disk form factor with the structure or form factor for some clay aggregate. A series of measurements on pure reference Laponite solutions at slightly different concentrations[10,15−17] above the gel transition (same pH and salt concentration) exhibit very similar behavior. In these cases it was very nicely demonstrated that the plateau region (slope of 0) includes a structure factor due to ordering between adjacent platelets. This is likely to be the case here as well. Because of the excess polymer, we cannot easily divide out the form factor to obtain the structure factor as done in the pure reference Laponite solutions.[10] However, by comparing our data to the reference data[10] and to some of our earlier work,[4,5] we can make a qualitative estimate of the scale of the interparticle correlation $d_{SANS} = 2\pi/q$ to be on the order of ca. 50−80 nm for all M_w's (with q on order 0.008−0.012 Å^{-1}).

The low q range in Figure 1a scales with $q^{-1.55}$ and confirms the presence of large scale structures. The large scale fractal structures in pure reference Laponite gels are quite dense with a slope of q^{-3}.[18] The significantly lower exponent measured here suggests that the polymer clay network form a much more open structure.

Figure 2 shows freeze fracture TEM images, from the network like polymer clay gel and cryo-TEM from a very

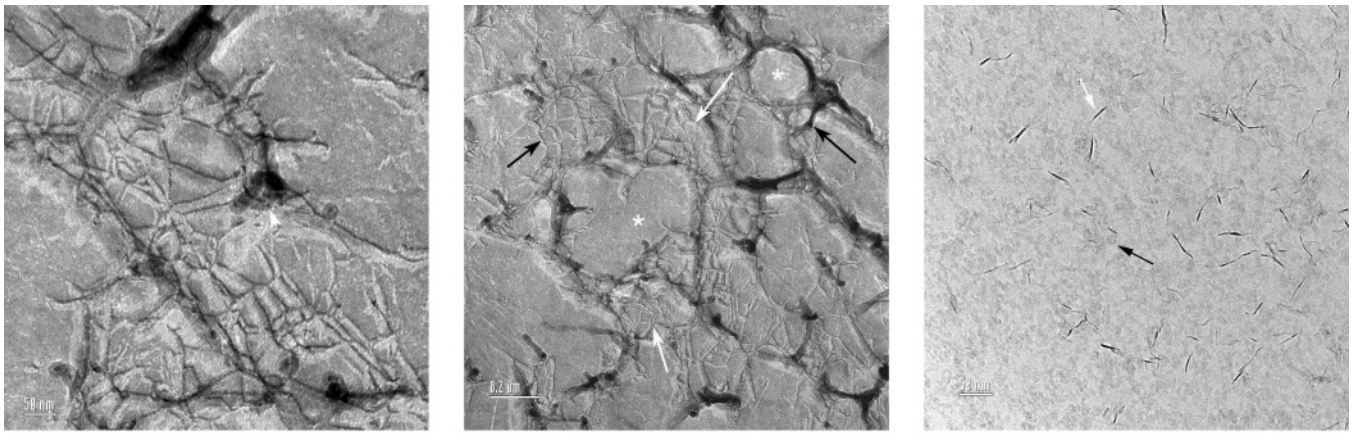

Figure 2. TEM: (a, b) Freeze fracture replicas of the polymer−clay hydrogel with polymer $M_w = 10^6$ g/mol, showing a network-like structure on a nanometer length scale. Arrows point to areas with network-like structure, and white asterisks indicate smooth areas. (c) Cryo-TEM from pure Laponite clay solution showing the thickness of single clay platelets visualized from the side. Arrows indicate single platelets. Scaling bar: (a) 50 nm, (b) 2.5 μm, and (c) 50 nm.

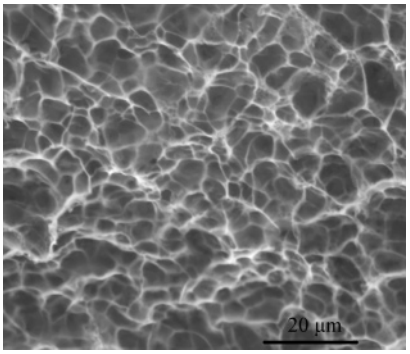

Figure 3. Representative SEM image of freeze fractured surfaces of a polymer−clay hydrogel with polymer $M_w = 10^6$ g/mol, showing the network-like structure on a micron length scale. Bright lines are clay-rich areas. Scaling bar: 20 μm.

dilute pure clay solution as reference showing the dimension of the individual clay platelets. The network like gel is characterized by an extremely fine texture of interconnected thin strings. The mesh size of the network is ca. 50−80 nm, in good agreement with the results obtained from SANS. The thickness of these strings is ca. 4 nm while the thickness of single clay platelets is ca. 1 nm. Interpreting these lines as polymer-coated platelets viewed from the side leads to an adsorbed layer thickness of 1.5 nm on each side, in perfect agreement with the values obtained from dilute solutions below the gel transition mentioned before.[10]

One should take care to overcome the natural tendency to overinterpret real space images. For example, for these freeze fracture samples we cannot see any platelets which do not happen to be sitting normal to the fracture plane, nor can we easily tell at what depth the observed platelets are. With these caveats, however, we may cautiously note that the platelets seem to lie within a network area adjacent to areas with no platelets. While there may be several interpretations for this, one consistent with conservation of volume arguments would be that in fact at these lengths scales the polymer coated platelets form a relatively tight network with hundreds of nanometer pockets of solution. Figure 2a,b also provides evidence that the clay platelets can interconnect by network-active polymer through their edges with many strings being much longer than the 30 nm nominal platelet diameter.

Although all samples are completely transparent to the eye and to optical microscopy, as are multilayered nanocomposite films made from the same polymer and clay components,[19] structures can be observed on a micron length scale using environmental scanning electron microscopy. Optical transparency of samples with micron size texture is usually possible when refractive index matching of the large scale structures is present. SEM, on the other hand, "sees" by reflection from the electron density and thus will clearly show areas of high electron density form the clay as bright areas while the low, and nearly equal (H_2O and H_2C are fairly similar in density), electron density will show up as darker regions (LRD contains many electron-rich atoms). In Figure 3, the SEM reveals an exquisite, lacey, spongelike texture on a micron length scale with on average 5 μm large clay-poor regions (dark areas) and ca. 1.5 μm thick interconnected membranes of clay-rich areas (bright lines). Several areas show fine network structures within the 5 μm size pores. Assuming the SEM and TEM interpretation is correct, this network like structure on the micron length scale is self-similar to that on the nanometer length scale observed by TEM (Figure 2a,b). Such an interpretation would be in excellent agreement with the open self-similar structure implied by the fractal dimension of 1.55 from the USANS which covers the same spatial range. Data obtained from a Fourier transformation of the real-space SEM image shown in Figure 3 are self-consistent with the USANS scattering data shown in Figure 1b.

By combining these techniques, the picture that begins to emerge for these strong gels from which meter long fibers can be drawn is one in which clay platelets covered by a 1.5 nm thick polymer coating are tethered together in fibrous bundles that form a very open fractal-like aggregate up into the micron regime. Confirmation of this picture, understanding the role of the excess polymer, and understanding to what extent the unique macroscopic properties are related to the above structure are part of our much larger ongoing effort requiring contrast matching techniques and studying how these characteristics change as a function of the various gelation parameters of concentration, ionic strength, polymer molecular weight, pH, and temperature.

Acknowledgment. This work was supported in part by an NSF-CAREER award, DMR 0348884. We also acknowledge the support of NIST and the NSF, through Agreement DMR 9986442, in providing the neutron research facilities used in this work. We thank Professor Henk from Louisiana State University, Veterinary School, for assistance with the SEM experiment and for many fruitful discussions. We thank Dr. Sheng Lin-Gibson for the USANS experiment.

References and Notes

(1) Schmidt, G.; Malwitz, M. M. *Curr. Opin. Colloid Interface Sci.* **2003**, *8*, 103−108.
(2) Gabriel, J. C. P.; Camerel, F.; Lemaire, B. J.; Desvaux, H.; Davidson, P.; Batail, P. *Nature (London)* **2001**, *413*, 504−508.
(3) Mongondry, P.; Nicolai, T.; Tassin, J. F. *J. Colloid Interface Sci.* **2004**, *275*, 191−196.
(4) Schmidt, G.; Nakatani, A. I.; Butler, P. D.; Han, C. C. *Macromolecules* **2002**, *35*, 4725−4732.
(5) Schmidt, G.; Nakatani, A. I.; Butler, P. D.; Karim, A.; Han, C. C. *Macromolecules* **2000**, *33*, 7219−7222.
(6) Schmidt, G.; Nakatani, A. I.; Han, C. C. *Rheol. Acta* **2002**, *41*, 45−54.
(7) Zebrowski, J.; Prasad, V.; Zhang, W.; Walker, L. M.; Weitz, D. A. *Colloids Surf. A* **2003**, *213*, 189−197.
(8) Lal, J.; Auvray, L. *Mol. Cryst. Liq. Cryst.* **2001**, *356*, 503−515.
(9) Lal, J.; Auvray, L. *J. Appl. Crystallogr.* **2000**, *33*, 673−676.
(10) Nelson, A.; Cosgrove, T. *Langmuir* **2004**, *20*, 2298−2304.
(11) Swenson, J.; Smalley, M. V.; Hatharasinghe, H. L. M.; Fragneto, G. *Langmuir* **2001**, *17*, 3813−3818.
(12) Smalley, M. V.; Hatharasinghe, H. L. M.; Osborne, I.; Swenson, J.; King, S. M. *Langmuir* **2001**, *17*, 3800−3812.
(13) Drews, A. R.; Barker, J. G.; Glinka, C. J.; Agamalian, M. *Physica B* **1997**, *241*, 189−191.
(14) Glinka, C. J.; Barker, J. G.; Hammouda, B.; Krueger, S.; Moyer, J. J.; Orts, W. J. *J. Appl. Crystallogr.* **1998**, *31*, 430−445.
(15) Pignon, F.; Magnin, A.; Piau, J. M. *Phys. Rev. Lett.* **1997**, *79*, 4689−4692.
(16) Kroon, M.; Vos, W. L.; Wegdam, G. H. *Phys. Rev. E* **1998**, *57*, 1962−1970.
(17) Kroon, M.; Vos, W. L.; Wegdam, G. H. *Int. J. Thermophys.* **1998**, *19*, 887−894.
(18) Bhatia, S.; Barker, J.; Mourchid, A. *Langmuir* **2003**, *19*, 532−535.
(19) Dundigalla, A.; Lin Gibson, S.; Ferreiro, V.; Malwitz, M. M.; Schmidt, G. *Macromol. Rapid Commun.* **2005**, *26*, 143−149.

MA047411A